Probing structural consequences of N9-alkylation in silver-adenine frameworks†

Ashutosh Kumar Mishra, Rajneesh Kumar Prajapati and Sandeep Verma*

Received 27th May 2010, Accepted 2nd September 2010
DOI: 10.1039/c0dt00557f

This communication explores the effect of varying substituent bulk at the N9 position of the adenine moiety and its effect in dictating the structural aspects of silver-adenine frameworks. While adenine alone or 9-benzyl substituted ligand afforded mono and dinuclear dimeric entities, *n*-propyl substitution at the N9 position results in the formation of a metallaquartet. Longer *n*-alkyl chains (hexyl and nonyl) resulted in the formation of linear polymeric chains, *via* N1 and N7 coordination.

Structural investigations of adenine-rich regions of DNA and RNA suggest that the adenine skeleton tends to favor various base interactions, including adenine tetrad formation.[1] In this context, designed oligonucleotide segments have been utilized to investigate hydrogen bonded structures of such adenine tetraplexes with the help of crystal structure, solution NMR, and theoretical calculations which suggest a bowl-like assembly for these adenine tetrads.[2]

Metal-mediated artificial base tetrads with a mixed-nucleobase regimen and involvement of two metal ions with a single nucleobase have also been reported in the literature, where hydrogen bonding interactions were replaced with coordinate bonds.[3] A family of silver mediated homoadenine metallaquartets involving four silver and four adenine moieties has been reported from our group, with a tridentate coordination mode *via* N1, N3 and N7 nitrogen atoms of modified adenine analogues.[4] Our investigation has led us to believe that subtle changes in the adenine skeleton and/or counter-anion do not affect the quartet formation. Furthermore, 9-substituted N6-connected bisadenine analogue also results in quartet formation with the involvement of four adenine and two silvers, while 9-functionalized adenine residues leads to silver-mediated hexad formation.[5]

We have been exploring metal-nucleobase complexes especially with copper and silver for various purposes ranging from polymer formation displaying catalytic and DNA cleavage activity, fluorescent sensors, generation of supramolecular architectures and their facile deposition on surfaces.[4–6] In continuation, we wish to systematically explore the metallaquartet formation which invariably reveals two inwardly projected N9 alkyl groups with smaller substituents (Scheme 1). Herein, we planned to perform solid state analysis of silver complexes of modified adenine analogues with varying substituents at the N9 position. For this,

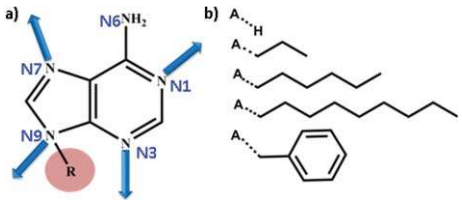

Scheme 1 (a) Schematic representation of the adenine moiety where arrows suggest possible sites for metal coordination. (b) Representation of varying substituents at the N9 position of the adenine moiety (where A stands for the adenine moiety).

we have prepared a silver complex of N9 unsubstituted adenine (**1**), revisited 9-propyladenine with perchlorate counteranion (**2**), with a longer alkyl chain at the N9 position namely hexyl (**3**) and nonyl (**4**), and with a benzyl group at the N9 position (**5**).

Crystallographic investigation of the silver complex of unsubstituted adenine, **1**, grown in acidic medium reveals a bidentate coordination mode for adenine resulting in dinuclear dimeric species (Fig. 1a). Each silver ion coordinates with N3 and N9 nitrogen of two different adenine molecules and two nitrate oxygens, thereby acquiring a distorted trigonal pyramidal geometry. The Ag···Ag bond distance is 3.08(11) Å, suggesting a strong argentophilic interaction, which corroborates well with a literature report for a similar adduct.[7]

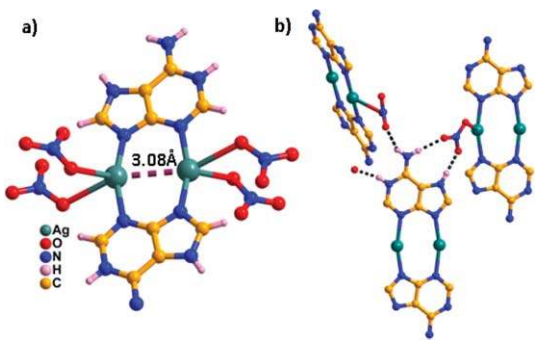

Fig. 1 (a) Dinuclear silver complex **1**, formed *via* N3 and N9 coordination. (b) Part of the crystal lattice showing hydrogen bonding interaction between the dimeric species. Part of the crystal lattice has been omitted for clarity.

Interestingly, the N6-hydrogen atom of the adenine residue is involved in intermolecular hydrogen bonding interactions with the nitrate groups while additional interaction is observed as a result of protonation at N1 and N7 nitrogens with water and nitrate, respectively (Fig. 1b). π–π stacking between the five membered rings of the adenine residue further stabilizes the crystal lattice, with the distance between the centroid of the two five membered rings being 3.55(7) Å (Fig. S1, ESI†).

Department of Chemistry, Indian Institute of Technology-Kanpur, Kanpur, 208016, (UP), India. E-mail: sverma@iitk.ac.in

† Electronic supplementary information (ESI) available: Experimental details. CCDC reference numbers 772592, 772591, 772587, 772589, and 767285 for complexes **1**, **2**, **3**, **4**, and **5**, respectively. For ESI and crystallographic data in CIF or other electronic format see DOI: 10.1039/c0dt00557f

As a move towards N9 substitution we introduced a *n*-propyl group to determine the effect of silver coordination. Crystallographic investigation of **2** reconfirms our previous observation of metallaquartet formation.[4] Crystals suitable for X-ray diffraction studies were obtained by a slow evaporation technique using an acetonitrile solution of **2**. Solid state analysis of **2** reveals the tridentate coordination mode *via* N1, N3 and N7 nitrogens of the adenine moiety, leading to metallaquartet formation with four silver atoms positioned at the corners of a distorted rectangle. The central part of the quartet comprises two inwardly projected N9 substituents and exocyclic N6 substituent from opposite ends (Fig. 2). Two different types of polymeric motifs are present in the crystal lattice; one with the participation of N3 and N7 and the other involving N1 and N3 coordination, giving rise to helical architectures (Fig. S2, ESI†).

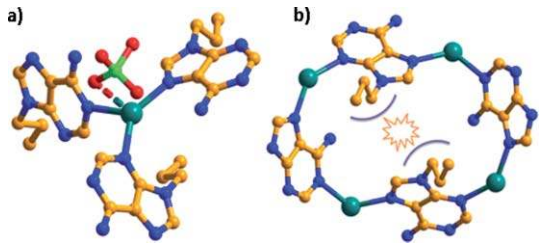

Fig. 2 (a) Silver complex-**2** showing tridentate coordination mode, (b) metallaquartet formation showing the possibility of steric compulsions involving inwardly projected alkyl groups.

The projection of the propyl group inside the metallaquartet cavity provided us with an impetus to increase the bulk of the alkyl group substituent at N-9, consequently, 9-hexyladenine (**3**) and 9-nonyl adenine(**4**) were prepared. Solid state investigation of silver complexes of **3** and **4** revealed a similar bidentate coordination mode for the adenine moiety *via* N1 and N7 nitrogen leading to a linear polymeric chain (Fig. 3a) where the hexyl/nonyl chains are flanked from both sides (Fig. S3, ESI†).

A closer inspection of the crystal lattice of **3**, suggests a T-shaped geometry around each silver ion formed *via* coordination with N1 and N7 of different adenine residues and nitrate oxygen. Notable differences have been observed for adjacent silver nitrate binding where the Ag–O bond distance and Ag–O–N angle varies from 2.59(8) to 2.82(1) Å and 164.47(1) to 110.14(9)°, respectively (Fig. S4, ESI†). Part of the crystal lattice when viewed along the *c*-axis reveals π–π stacking interactions between the adenine moieties giving further stability to the crystal lattice. The distance between the centroids of the two six membered rings is ~ 3.62(2) Å (Fig. 4a).

Crystallographic investigation of **4** reveals a similar bidentate coordination mode for the adenine moiety leading to a linear polymeric chain; however two crystallographically unique silver ions, **Ag1** and **Ag2** were observed in the crystal lattice. While **Ag1** acquires T-shaped geometry around the silver ion by coordinating with two nitrogen atoms from two different adenine moieties and an oxygen atom from the nitrate anion; the adjacent silver, **Ag2** coordinate with two different adenine residues and two nitrate groups, thereby acquiring a distorted tetrahedral geometry (Fig. 3c).

A unique binding mode has also been observed for nitrate oxygen; where in the case of **Ag1** it gets coordinated as an oxido group while with **Ag2** it exits as a μ-oxido connecting two **Ag2**

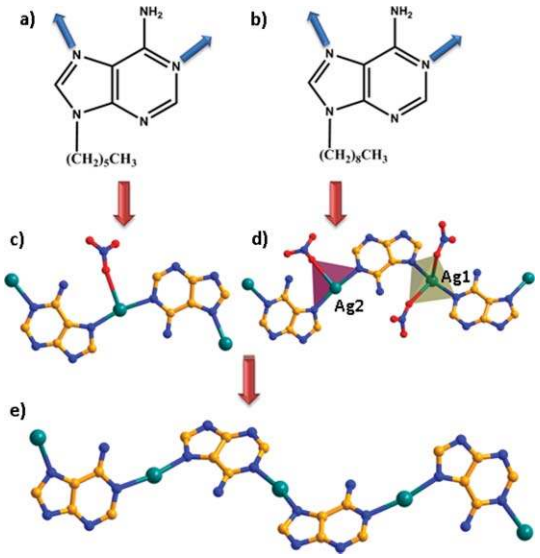

Fig. 3 (a) and (b) Chemical structures of 9-hexyl and 9-nonyladenine, where arrows show the actual coordination sites in complexes. (c) T-shaped geometry around the Ag^+ ion in **3**. (d) Coordination geometries of two crystallographically different Ag^+ ions, namely Ag1 and Ag2, in **4**. (e) Representation of a linear polymeric chain formed in **3** and **4** *via* N1 and N7 coordination.

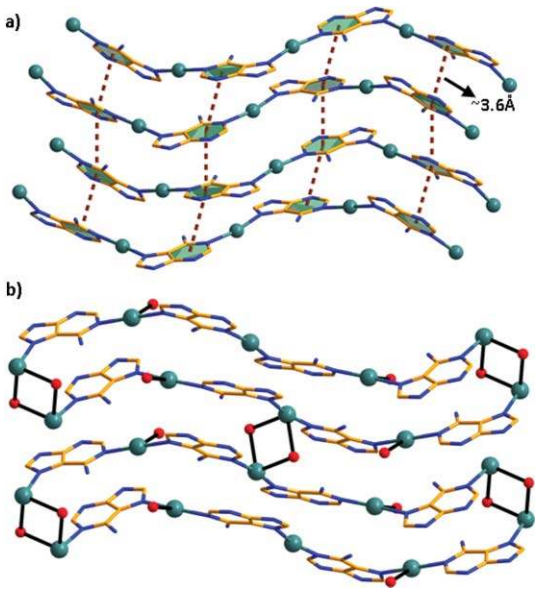

Fig. 4 (a) Part of the crystal lattice in **3** showing π–π stacking interaction. (b) Representation of interconnected polymeric chains *via* a nitrate bridge in **4**, resulting in 3-D lattice formation (oxygen atoms are from nitrate groups).

ions from different polymeric chains resulting in the formation of a 3D polymeric network. The Ag–O bond distance and Ag–O–Ag angle are ~2.69(6) Å and 83.29(1)°, respectively.

The nitrate bridge connecting the two polymeric chains brings the adenine moieties in close proximity thereby resulting in π–π stacking interactions between the adenine moieties. The distances between the centroids of the six membered ring of the stacked adenine moiety are in the range of 3.53(5) to 3.68(6) Å.

Introduction of an aromatic phenyl ring at the N9 position of adenine leads to 9-benzyladenine (**5**), exhibiting a monodentate coordination mode *via* N1 alone resulting in a dimeric silver complex. Such an arrangement is rarely observed for adenine thus, there are very few reports depicting the N1–M–N1 coordination mode for the adenine moiety.[8]

The asymmetric unit consists of silver ion coordinated to N1 nitrogens of two adenine moieties while the other two coordination sites were occupied by a nitrate oxygen and an acetonitrile molecule, thus acquiring a distorted tetrahedral geometry around the silver ion. N6-hydrogen atoms of the adenine moiety are involved in the hydrogen bonding with nitrate oxygen as well as the N7 nitrogen of the adjacent adenine. Additionally, intermolecular hydrogen bonding interactions between the oxygen atoms of the nitrate anion and the C8-H of the adjacent adenine molecules further stabilizes the crystal lattice (Fig. 5).

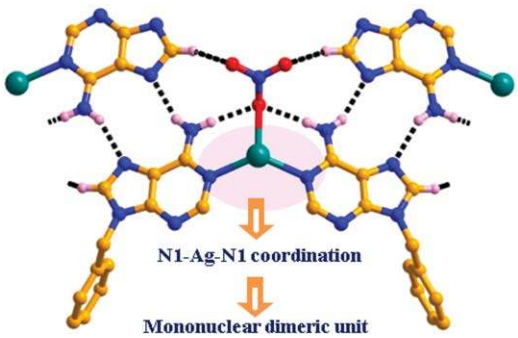

Fig. 5 Part of the crystal lattice showing hydrogen bonding interactions (dotted lines) between N6-H and C8-H of the adenine moiety with nitrate oxygen along with N6-H with N7 nitrogen of the adenine moiety. Highlighted portion reveals monodentate coordination mode for the adenine moiety resulting in mononuclear dimeric species.

Part of the crystal lattice when viewed along the *c*-axis reveals extensive π–π stacking interactions between the adjacent adenine moieties where the distance between the centroids of the adenine units is found to be 3.56(6) Å (Fig. S5, ESI†). Significant stacking interaction has also been observed between adjacent benzyl substituents, thereby stabilizing the crystal lattice.

In conclusion, we have systematically explored the silver-adenine coordination mode with varying substituents at the N9 position. Scheme 2 represents the variation in coordination sites resulting in different structural patterns, in N9-substituted adenine-silver complexes. While smaller substituents at the N9 position results in a unique μ-N1,N3,N7 coordination mode leading to metallaquartet formation, larger substituents affect the coordination mode to afford either linear chain *via* N1 and N7 coordination or a dimeric species with rare N1–Ag–N1 coordination. These results may be helpful in understanding the binding of silver ion with nucleic acids, leading to conformational transitions.

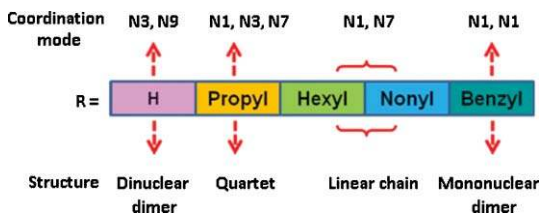

Scheme 2 Pictorial representation of the varying complexity of silver adenine complexes as a result of N9 substitution.

X-Ray crystal data were collected on a Bruker SMART APEX CCD diffractometer instrument using graphite-monochromated Mo KR radiation ($\lambda = 0.71073$). The hexyl and nonyl chains in **3** and **4** are disordered and solved by using various restraints, like DFIX, ISOR *etc*. All non-hydrogen atoms are refined anisotropically and hydrogen atoms are placed at geometrically idealized position. Crystal data for **1**: $C_{10}H_{12}Ag_2N_{14}O_{14}$, M = 768.08, Monoclinic, a = 6.5283(17), b = 8.175(2), c = 20.896(5) Å, β = 95.687(4), U = 1109.7(5) Å^3, T = 100(2) K, space group = $P2_1/c$ (no. 14), Z = 2, 6942 reflections measured, 2727 unique (R_{int} = 0.0390) which were used in all calculations. R_1 = 0.0440 ($I > 2\sigma(I)$)], The final $wR(F_2)$ was 0.1870 (all data). Crystal data for **2**: $C_8H_{11}AgClN_5O_{4.5}$, M = 392.54, Orthorhombic, a = 25.146(5), b = 25.516(4), c = 7.849(3), U = 5036(2) Å^3, T = 100(2) K, space group = $Fdd2$ (no. 43), Z = 16, Flack parameter = –0.18(11), 7959 reflections measured, 2683 unique (R_{int} = 0.0533) which were used in all calculations. R_1 = 0.0498($I > 2\sigma(I)$), The final $wR(F_2)$ was 0.1987 (all data). Crystal data for **3**: $C_{39}H_{57}Ag_4N_{24}O_{16}$, M = 1549.57, Monoclinic, a = 18.577(4), b = 7.346(5), c = 25.747(3), β = 103.013(5), U = 3423(3) Å^3, T = 100(2) K, space group = $P2_1/c$ (no. 14), Z = 2, 21565 reflections measured, 8482 unique (R_{int} = 0.1001) which were used in all calculations. R_1 = 0.0997($I > 2\sigma(I)$), The final $wR(F_2)$ was 0.3383 (all data). Crystal data for **4**: $C_{55}H_{91}Ag_4N_{24}O_{16}$, M = 1776.00, Monoclinic, a = 20.600(3), b = 7.1530(11), c = 25.954(4), β = 93.326(5), U = 3817.9(10) Å^3, T = 100(2) K, space group = $P2_1/c$ (no. 14), Z = 2, 23423 reflections measured, 9349 unique (R_{int} = 0.0692) which were used in all calculations. R_1 = 0.0749($I > 2\sigma(I)$),The final $wR(F_2)$ was 0.2242 (all data). Crystal data for **5**: $C_{26}H_{25}AgN_{12}O_3$, M = 661.45, Orthorhombic, a = 23.072(4), b = 19.976(5), c = 6.025(4), U = 2777(2) Å^3, T = 100(2) K, space group = $Pnma$ (no. 62), Z = 4, 14489 reflections measured, 2818 unique (R_{int} = 0.0690) which were used in all calculations. R_1 = 0.0404($I > 2\sigma(I)$), The final $wR(F_2)$ was 0.1197 (all data).

Caution! Perchlorate salts are potentially hazardous, and should be handled with care.

Notes and references

1 (*a*) B. Pan, Y. Xiong, K. Shi, J. Deng and M. Sundaralingam, *Structure*, 2003, **11**, 815; (*b*) B. Pan, Y. Xiong, K. Shi and M. Sundaralingam, *Structure*, 2003, **11**, 825.

2 (*a*) V. Esposito, A. Randazzo, A. Galeone, M. Varra and L. Mayol, *Bioorg. Med. Chem.*, 2004, **12**, 1191; (*b*) E. Gavathiotis and M. S. Searle, *Org. Biomol. Chem.*, 2003, **1**, 1650; (*c*) P. K. Patel, A. S. Koti and R. V. Hosur, *Nucleic Acids Res.*, 1999, **27**, 3836; (*d*) J. Suhnel, *Biopolymers*, 2001, **61**, 32; (*e*) J. Gu and J. Leszczynski, *Chem. Phys. Lett.*, 2001, **335**, 465.

3 (*a*) P. Amo-Ochoa, P. J. S. Miguel, P. Lax, I. Alonso, M. Roitzsch, F. Zamora and B. Lippert, *Angew. Chem., Int. Ed.*, 2005, **44**, 5670; (*b*) B. Knobloch, R. K. O. Sigel, B. Lippert and H. Sigel, *Angew. Chem., Int. Ed.*, 2004, **43**, 3793.

4 (*a*) C. S. Purohit, A. K. Mishra and S. Verma, *Inorg. Chem.*, 2007, **46**, 8493; (*b*) C. S. Purohit and S. Verma, *J. Am. Chem. Soc.*, 2006, **128**, 400.

5 (*a*) A. K. Mishra, C. S. Purohit and S. Verma, *CrystEngComm*, 2008, **10**, 1296; (*b*) J. Kumar and S. Verma, *Inorg. Chem.*, 2009, **48**, 6350.

6 (*a*) C. S. Purohit and S. Verma, *J. Am. Chem. Soc.*, 2007, **129**, 3488; (*b*) A. K. Mishra and S. Verma, *Inorg. Chem.*, 2010, **49**, 3691; (*c*) M. D. Pandey, A. K. Mishra, V. Chandrasekhar and S. Verma, *Inorg. Chem.*, 2010, **49**, 2020; (*d*) S. G. Srivatsan and S. Verma, *Chem. Commun.*, 2000, 515; (*e*) S. Verma, A. K. Mishra and J. Kumar, *Acc. Chem. Res.*, 2010, **43**, 79; (*f*) R. K. Prajapati, J. Kumar and S. Verma, *Chem. Commun.*, 2010, **46**, 3312; (*g*) S. G. Srivatsan and S. Verma, *Chem.–Eur. J.*, 2001, **7**, 828; (*h*) S. G. Srivatsan and S. Verma, *Chem.–Eur. J.*, 2002, **8**, 5184.

7 C. Gagnon, J. Hubert, R. Rivest and A. L. Beauchamp, *Inorg. Chem.*, 1977, **16**, 2469.

8 (*a*) B. Longato, L. Pasquato, A. Mucci and L. Schenetti, *Eur. J. Inorg. Chem.*, 2003, 128; (*b*) B. Longato, L. Pasquato, A. Mucci, L. Schenetti and E. Zangrando, *Inorg. Chem.*, 2003, **42**, 7861.